APPENDIX

A.1 Experimental Generation of Tunable Vacuum Ultraviolet Light

A systematic approach for the selection and generation of vacuum ultraviolet (VUV) light is presented below followed with a description of each step in detail for an example experiment to generate 9.60 eV light.

1. Acquire the ionization (IE) energies of your molecules of interest such as molecules A and B with ionization energies IE(A) and IE(B). Then select the wavelengths that will discriminate individual isomers based upon their IEs to determine the isomer's contribution to the signal.

2. Determine if non-resonant (10.49 eV) and/or resonant four-wave sum or difference mixing can generate the necessary wavelengths (ω_{vuv}) based on the possible resonance states of krypton and/or xenon by exploiting the "VUV Calculator" program.

3. If the ω_{vuv} light is accessible via four-wave mixing, the laser system wavelength ranges need to be checked to make sure that the selected process is feasible (dye laser range, organic dyes, BBO crystals, mirrors, LiF lens).

4. Once an acceptable VUV generation scheme has been chosen, the respective Nd:YAG and Sirah dye laser manuals should be consulted for correct operation to produce the necessary wavelengths as determined from the previous steps.

5. After the visible and/or UV light has been generated, they have to be spatially overlapped, utilizing prisms and/or mirrors, and centered through two adjustable apertures. The different wavelengths are also temporally overlapped using a pulse delay generator.

6. The overlapped beams are then focused via a UV grade fused silica plano-convex lens through a UV grade fused silica window into a T extension connected to a pulsed valve, where the krypton or xenon gas jet is emitted.

7. The light passing through/produced in the gas is then separated with a lithium fluoride (LiF) bi-convex lens based on the relative refractive index (A.3). This lens also focuses the desired wavelength in front of the substrate where molecules are subliming, and aligns the beam to the detector. Undesired wavelengths are eliminated.

8. Two detectors are utilized to measure the photon flux. Initially a faraday cup is utilized to observe and maximize the intensity of the VUV signal from alignment of the optical elements. Then, a NIST calibrated photodiode is used to measure the photon flux of the VUV light. The faraday cup is the detector utilized to monitor the VUV intensity online during an experiment.

STEP 1:

The initial step is to determine the IE of your molecule(s) of interest. The experimentally determined ionization energy of molecules can be extracted from two databases: https:// web-book.nist.gov/chemistry/ and http://flame.nsrl.ustc.edu.cn/database/data.php. When utilizing these databases or SciFinder, take notice of what method was utilized in determining the value and use IE values extracted from photoionization (PI) over alternative ionization techniques such as electron impact (EI). Furthermore, the IE utilized must be the adiabatic; reference spectra should be checked, when available, to determine the exact onset value of the IE. An extensive literature search (SciFInder) may be needed to acquire the true adiabatic IE for the molecule(s) of interest. Once the IE has been acquired, accessible photon energies must be selected to separate the contribution of different isomers.

STEP 2:

In order to photoionize subliming molecules in the present experiments, pulsed (30 Hz), coherent VUV light can be utilized. By altering the energy of the photons used, the isomer specific detection of a molecule can be confirmed or eliminated. Therefore, not only is the IE of the molecule(s) of interest needed, but also the IEs of the isomers. It is important to point out that the wavelengths needed to be generated are typically in the VUV range (5.0 – 11.0 eV) and would not transmit through a β-BaB_2O_4 (BBO) crystal of the lasers because the BBO crystal would absorb the light. Therefore, the dissertation experiments produced VUV photons via both resonant and non-resonant four-wave mixing in pulsed xenon or krypton gas, see section A.2 for the mathematical derivation of the four-wave mixing process.

Non-resonant four-wave mixing was utilized to produce 10.49 eV photons (118 nm). In detail, the 10.49 eV photons were generated by exploiting the third harmonic (354.6 nm; 3.490 eV) of the 1063.8 nm (1.162 eV) fundamental of a Nd:YAG laser (Spectra Physics, PRO-250-30); the 354.6 nm (3.490 eV; 333 mJ per pulse) photon is then frequency tripled ($\omega_{vuv} = 3\omega_1$; Figure A.1.1, left) using pulsed jets of xenon as a non-linear medium (80 μs, 30 Hz) with 1,550 Torr backing pressure to produce 118.2 nm (10.49 eV) light via non-resonant mixing (Figures A.1.1-A.1.7).[1] Typically non-resonant four-wave mixing is less intense, but due to the high output of the Nd:YAG laser, the 118 nm wavelength can be produced at fluxes as high as $\mathbf{1 \times 10^{12}}$

photons s^{-1}. This process is often selected initially as it is easier to produce VUV light from a single input beam. Utilizing a single laser is a simpler setup as there is no need to account for overlap of multiple lasers in space or time, as will be necessary for resonant four-wave mixing which is discussed next.

Considering resonant four-wave mixing, the wavelength range of the generated VUV light (ω_{vuv}) is related to the accessed resonance line of the non-linear mixing medium. Recall that the resonance state reflects an excited state of the atom. Rare gases such as krypton and xenon are popular non-linear media used here as these have well-established resonance lines, i.e. a spectral line of the radiation from an atom at a frequency that coincides with the frequency of the light absorbed by the atom in its ground state, that are easily obtainable by a two photon process ($2\omega_1$); this can then be added to or subtracted by a second photon (ω_2). Here, "$2\omega_1$" corresponds to the sum of two ω_1 photons ($\omega_1 + \omega_1 = 2\omega_1$). Figure A.1.1 shows the resonant four-wave sum mixing (middle) and resonant four-wave difference mixing (right). The resonant four-wave difference mixing exploiting two photons of ω_1 and one photon of ω_2, i.e. $2\omega_1 - \omega_2$, was used to produce all wavelengths, except 118 nm (10.49 eV), discussed in the dissertation.[2, 3]

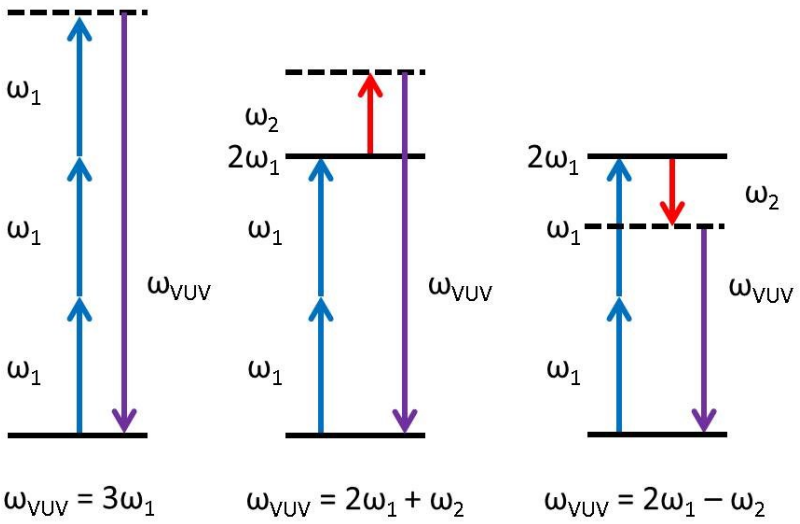

Figure A.1.1. Schematic of the four-wave mixing process to produce VUV photons. The blue arrows represent wavelength one (ω_1), red arrows correspond to the second wavelength used (ω_2), and purple arrows designate the VUV photon that is produced (ω_{VUV}). Non-resonant four-wave mixing is shown on the left, while resonant four-wave sum and difference mixing are shown in the middle and right, respectively. **Typically, ω_1 is in the UV range, whereas ω_2 is in the VIS range.**

For example 9.60 eV photons were produced via four-wave difference mixing ($\omega_{vuv} = 2\omega_1 - \omega_2$). Figure A.1.2 shows the "VUV calculator" program with the "VUV Mixing" tab selected (left upper corner); this program was utilized to determine the wavelength values needed to generate 9.60 eV photons. This program is installed on the Keck apparatus computer and can be accessed or downloaded from its hard drive. The following steps are in reference to the "VUV calculator" program and Figure A.1.2. On the left side of the program (black box; Figure A.1.2) are the different units of the input and output values, and the identity of each value is listed at the top of these columns ($2\omega_1$, ω_2, VUV). Here, the "$2\omega_1$" column values correspond to the wavenumber (ω; cm^{-1}), wavelength (λ; nm), and energy (E; eV) of the light needed to access the resonant state of the krypton or xenon gas selected. Recall that multiplication or division of a photon's frequency or energy results in the inverse operation to its wavelength. Next, the different accessible resonant states in these gases are found in the dropdown menu (blue box; Figure A.1.2). The "ω_2" column values correspond to the wavenumber (cm^{-1}), wavelength (nm), and energy (eV) of the light needed to tune the energy of the VUV photon produced from four-wave mixing, which is shown in the third column labeled "VUV", by either adding or subtracting from the energy of the resonant state of the krypton or xenon gas selected, which are termed resonant sum ($\omega_{vuv} = 2\omega_1 + \omega_2$; orange box; Figure A.1.2) and four-wave difference ($\omega_{vuv} = 2\omega_1 - \omega_2$; green box; Figure A.1.2) mixing, respectively. A walkthrough on the selection of the laser setups possible and ultimately chosen to generate 9.60 eV photons follows (Figures A.1.1-A.1.7).

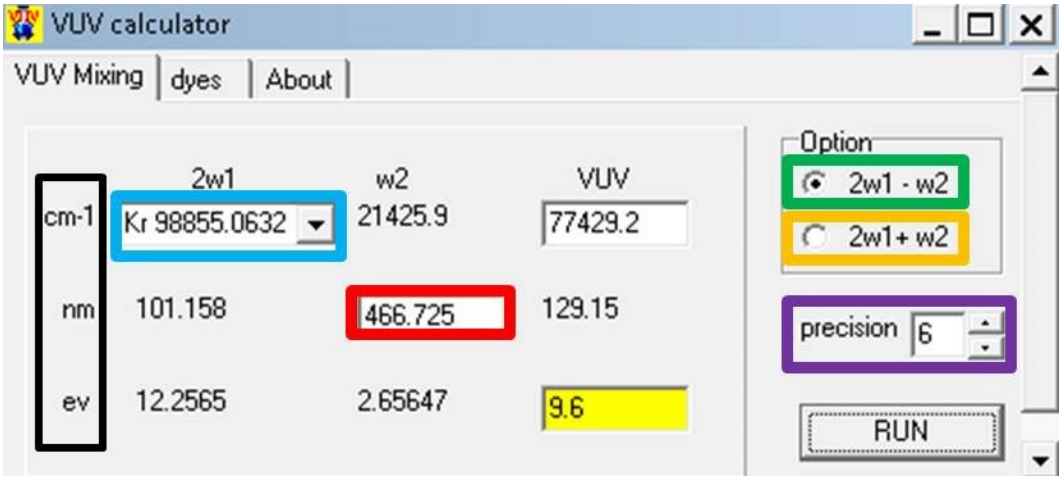

Figure A.1.2. The "VUV calculator" program showing the necessary wavelengths for resonant four-wave mixing production of VUV photons via a gas resonance (see text for details).

1. Start the VUV calculator program and enter the photon energy of interest (9.6 eV) – see yellow box in Figure A.1.2.

2. Select the resonant four-wave mixing process to be used under "Option", either resonant four-wave **difference** mixing (green box, Figure A.1.2) or resonant four-wave **sum** mixing (orange box, Figure A.1.2). Typically the difference option is chosen due to its higher efficiency. If the difference option cannot produce the desired photon energy , select the sum mixing option.

3. Set the precision to "6" since this will provide values with precision as low as picometers, which is the precision range of the wavemeter utilized to measure the laser wavelengths.

4. Select the very first krypton resonance line "Kr 94092.8557" from the dropdown menu (blue box; Figure A.1.2).

5. Click "RUN" and record all values generated as in Table A.1.1.

6. Select not the second resonance line from the program and again record the output values. Repeat this step until all five resonance lines have been accounted for and their outputs have been recorded. This will yield a Table similar to Table A.1.1a.

7. Calculate the value of ω_1 for each scheme. Recall that this means multiplying the wavelength by two or dividing the energy by a factor of two.

Table A.1.1. Overview of VUV Selection Process to Generate 9.60 eV Photons via $2\omega_1 - \omega_2$

(a) Resonance	**$2\omega_1$**		**ω_2**	
Kr 94092	106.278 nm	11.666 eV	600.108 nm	2.06603 eV
Kr 98855	101.158 nm	12.257 eV	466.725 nm	2.65647 eV
Kr 103761	96.3747 nm	12.865 eV	379.760 nm	3.26481 eV
Xe 80119	124.814 nm	9.9335 eV	3717.19 nm	0.333543 eV
Xe 89860	111.283 nm	11.141 eV	804.414 nm	1.54130 eV
Resonance	**ω_1 (UV range)**		**ω_2 (VIS range)**	
Kr 94092	212.54 nm	5.83 eV	600.108 nm	2.06603 eV
Kr 98855	202.30 nm	6.15 eV	466.725 nm	2.65647 eV
Kr 103761	192.74 nm	6.43 eV	379.760 nm	3.26481 eV
Xe 80119	249.62 nm	4.96 eV	3717.19 nm	0.333543 eV
Xe 89860	222.56 nm	5.57 eV	804.414 nm	1.5413 eV
	ω_1 (check accessible BBO range)		**ω_2 (check accessible dye range)**	

⬇

(b) Resonance	**ω_1**		**ω_2**	
Kr 98855	202.316 nm	6.128 eV	466.725 nm	2.656 eV
Xe 89860	222.566 nm	5.571 eV	804.414 nm	1.541 eV

⬇

BBO Crystal Selection for ω_1		
SHG-215: 215 – 280 nm (Frequency Doubling)	SHG-250: 250 – 380 nm (Frequency Doubling)	THG-197: 197 – 210 nm (Frequency Tripling)

⬇

Dye Laser Selection for ω_1 and ω_2	
$\frac{\omega_1}{3}$ = 606.948 nm (2.04 eV)	ω_2 = 466.725
Dye Laser #1 Wavelength Range	Dye Laser #2 Wavelength Range
350-630 nm	400-900 nm

⬇

Resonance	**$\frac{\omega_1}{3}$**		**ω_2**	
Kr 98855	606.948 nm	2.04 eV	466.725 nm	2.05 eV

⬇

Final Selected Parameters								
	$\frac{\omega_1}{3}$				**ω_2**			
Gas	YAG 1	Dye 1	Wavelength	Energy	YAG 2	Dye 2	Wavelength	Energy
Kr	532 nm	Mix. Rh 610/ Rh 640	606.948 nm (THG-197)	2.04 eV	355 nm	Coumarin 460	466.725 nm	2.66 eV

Notes: [a] Ranges of other optical elements: Fused silica lens/window: 180 – 2100 nm or 6.88 – 0.59 eV; LiF lens: 105 – 6000 nm or 11.8 – 0.20 eV.

STEP 3:

Now that the theoretical photons needed (ω_1, ω_2) for each VUV generation scheme have been determined (Table A.1.1a), the user has to see which of these five wavelength combinations can be actually generated by the laser setup. This is constrained based on the laser system wavelength capabilities. For ω_1, this is dictated first by the range of the doubling and tripling crystals to generate ω_1 from $\omega_1/2$ (SHG; doubling) or $\omega_1/3$ (THG; tripling), respectively (Table A.1.2) and the range of the dye laser 1 (350 – 630 nm) – in this case to generate $\omega_1/2$ or $\omega_1/3$; for ω_2, this is limited by the range of the dye laser 2 (400 – 900 nm) to generate ω_2.

Table A.1.2. Inventory of BBO Crystals [a]

BBO Crystal	Angle	Wavelength Range ω_1 (nm)
THG-197	77.0º	197 – 210
SHG-250	44º	250 – 380
SHG-215	57.4º	215 – 280

Notes: [a] BBO is an abbreviation for β-BaB_2O_4 and the angle refers to the optical axis of the crystal allowing for the optimal phase matching conditions. SHG: second harmonic generation (doubling); THG: third harmonic generation (tripling)

1. Check if ω_1 can be generated in laser system 1 (Nd:YAG 1 pumped dye laser 1; UV system). For this you have to see if one of the BBO crystals can produce ω_1 by doubling or tripling as the BBO crystals available in the laser have limited wavelengths (Table A.1.2). Based on these ranges, the first and third krypton schemes are not feasible (red highlight Table A.1.1a).

2. Check if ω_2 can be generated in laser system 2 (Nd:YAG 2 pumped dye laser 2; VIS system). Any schemes with ω_2 values outside the range of 400-900 nm can be eliminated (red highlight Table A.1.1) as each dye laser has a limited range (dye laser #1: 350 – 630 nm; dye laser #2: 400 – 900 nm). This reduces Table A.1.1a to table A.1.1b.

3. If multiple schemes are still possible to generate the wavelength needed, choose the scheme that will utilize dyes with the highest efficiency (Figure A.1.3). This can be calculated from ω_1 and from ω_2. The ω_1 wavelengths can be produced by either frequency doubling (SHG) of $\omega_1/2$ or tripling (THG) of $\omega_1/3$ via BBO crystals (Table A.1.2) of the wavelength of dye laser 1; the dye laser wavelength, which is needed to access each possible wavelength $\omega_1/2$ or $\omega_1/3$, is compiled in Table A.1.3. IMPORTANT: The ω_2 wavelengths are produced directly from the dye laser and Figure A.1.3 can be directly consulted.

Table A.1.3. BBO UV generation schemes

ω_1 (nm)	Frequency Conversion Process	BBO Crystal	Dye Laser Wavelength (nm)
202.316	Tripling	THG-197	606.948
222.566	Doubling	SHG-215	445.132

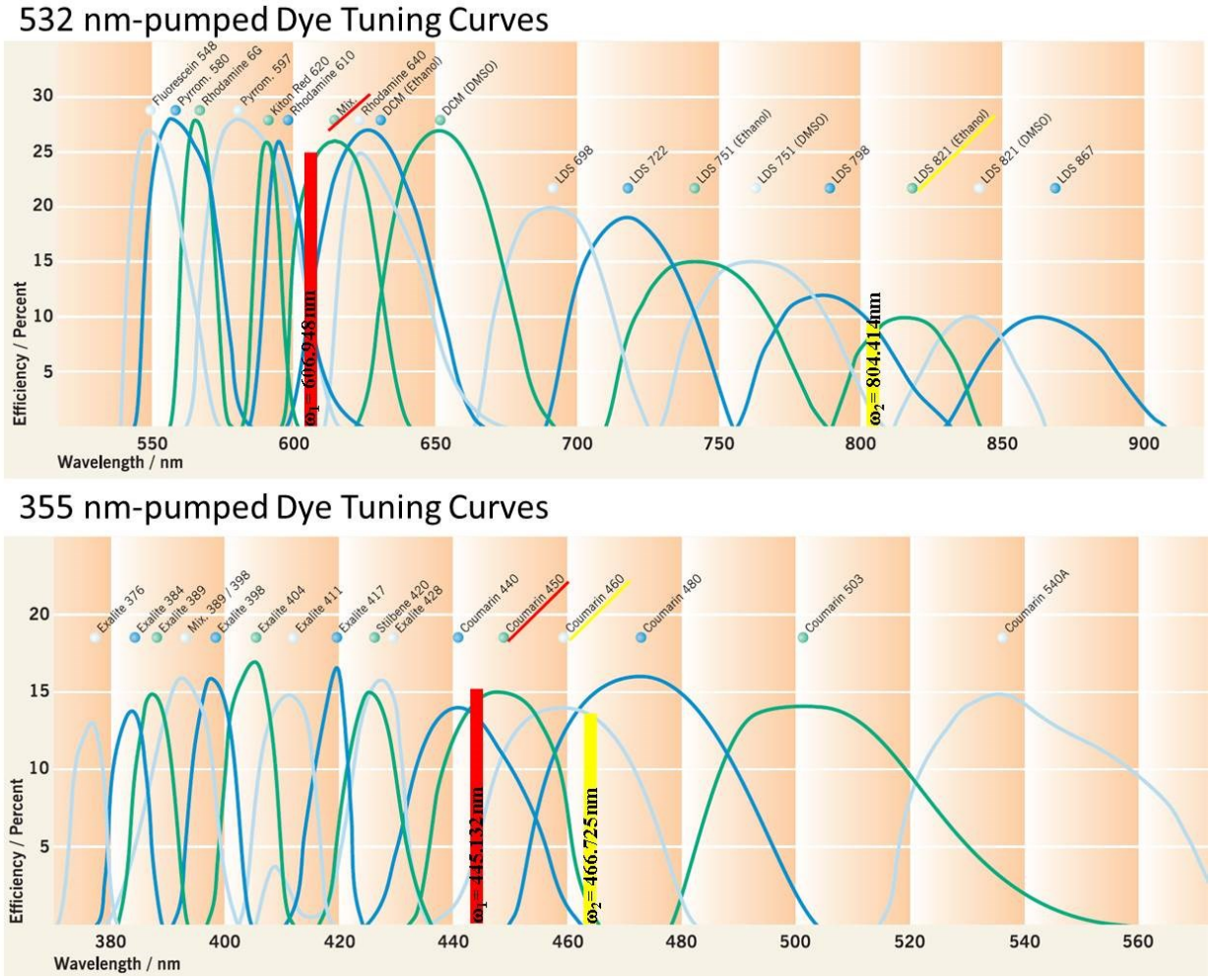

Figure A.1.3. Range of 532 and 355 nm pumped dye wavelengths (http://www.sirah.com/).

Which of the two pathways is more efficient to generate 9.60 eV (Table A.1.1b)? Here, the dye wavelengths needed for the ω_1 photons are 606.948 nm and 445.132 nm (Table A.1.3), which have dye efficiencies of about 25 % and 15 %, respectively (red, Figure A.1.3). The dye efficiency for the ω_2 photons at 466.725 nm and 804.414 nm are 15 % and 8%, respectively (yellow, Figure A.1.3). Considering Table A.1.1b, this gives a combination of 25 % and 15 % (Kr 98855) versus 15 % and 8 % (Xe 89860). Therefore, the krypton generation scheme has higher dye efficiencies for both the ω_1 and ω_2 photons and was chosen for the experimental setup

(green highlight, Table A.1.1b). It is important to highlight that dyes can have different solvents such as methanol (CH_3OH), ethanol (C_2H_5OH), or dimethylsulfoxide (DMSO). For convenience and lower toxicity, methanol (CH_3OH) and ethanol (C_2H_5OH) are preferred (Table A.1.4; www.exciton.luxottica.com) Since the dye laser is pumped by a Nd:YAG laser, which can be operated at 355 nm and 532 nm, we have to decide based on the dyes (Figure A.1.3) at which wavelength the Nd:YAG laser is operated. This reveals that for the ultimate generation of ω_1, Nd:YAG laser 1 has to be operated at 532 nm; to eventually generate ω_2, Nd:YAG laser 2 has to be operated at 355 nm.

Table A.1.4. Dye Solution Specifications[a] Notes: [a] (http://www.sirah.com/).

532 nm-pumped dyes

Name	Peak (nm)	Range (nm)	Efficiency	Solvent	Concentration (gram/liter)	Comment
Fluorescein 548	550	541 .. 571	27 %	Ethanol + H_2O	0.40	+ 0.2 g/l NaOH
Pyrromethene 580	557	547 .. 581	28 %	Ethanol	0.20	
Rhodamine 590	566	559 .. 576	28 %	Ethanol	0.09	Rhodamine 6G
Pyrromethene 597	582	566 .. 611	28 %	Ethanol	0.16	
Kiton Red 620	591	585 .. 600	26 %	Ethanol	0.20	Sulforhodamine B
Rhodamine 610	596	588 .. 614	26 %	Ethanol	0.20	Rhodamine B
Mix. Rh 610 / Rh 640	615	598 .. 636	26 %	Ethanol	0.17 / 0.04	
Rhodamine 640	624	614 .. 662	25 %	Ethanol	0.25	Rhodamine 101
DCM	627	602 .. 660	27 %	Ethanol	0.30	
DCM	651	626 .. 685	27 %	DMSO	0.30	
LDS 698	692	667 .. 720	20 %	Ethanol	0.25	Pyridine 1
LDS 722	718	691 .. 751	19 %	Ethanol	0.25	Pyridine 2
LDS 751	744	712 .. 782	15 %	Ethanol	0.15	Styryl 8
LDS 751	764	733 .. 802	15 %	DMSO	0.15	Styryl 8
LDS 798	785	758 .. 826	12 %	Ethanol	0.14	Styryl 11
LDS 821	815	791 .. 839	10 %	Ethanol	0.13	Stryryl 9
LDS 821	839	814 .. 862	10 %	DMSO	0.13	Styryl 9
LDS 867	863	832 .. 900	10 %	Ethanol	0.15	

355 nm-pumped dyes

Name	Peak (nm)	Range (nm)	Efficiency	Solvent	Concentration (gram/liter)	Comment
Exalite 376	377	372 .. 380	13 %	p-Dioxane	0.90	
Exalite 384	384	379 .. 388	14 %	p-Dioxane	0.30	
Exalite 389	387	382 .. 392	15 %	p-Dioxane	0.20	
Mix. Exalite 389 / 398	393	382 .. 401	16 %	p-Dioxane	0.10 / 0.10	
Exalite 398	398	393 .. 403	16 %	p-Dioxane	0.18	
Exalite 404	405	399 .. 410	17 %	p-Dioxane	0.15	
Exalite 411	411	404 .. 417	15 %	p-Dioxane	0.14	
Exalite 417	419	413 .. 422	17 %	p-Dioxane	0.20	
Stilbene 420	425	419 .. 434	15 %	Ethanol + H_2O	0.22	Stilbene 3
Exalite 428	427	419 .. 434	16 %	p-Dioxane	0.15	
Coumarin 440	441	429 .. 460	14 %	Ethanol	0.25	Coumarin 120
Coumarin 450	448	434 .. 463	15 %	Ethanol	0.20	Coumarin 2
Coumarin 460	460	442 .. 479	14 %	Ethanol	0.25	Coumarin 47
Coumarin 480	473	452 .. 500	16 %	Ethanol	0.40	Coumarin 102
Coumarin 503	500	480 .. 540	14 %	Ethanol	0.40	Coumarin 307
Coumarin 540A	535	517 .. 574	15 %	Ethanol	1.60	Coumarin 153
Rhodamine 590	574	563 .. 597	14 %	Ethanol	0.40	Rhodamine 6G
Pyrromethene 597	585	571 .. 612	12 %	Ethanol	0.32	
Kiton Red 620	596	582 .. 620	13 %	Ethanol	0.30	Sulforhodamine B
Rhodamine 610	600	588 .. 632	13 %	Ethanol	0.35	Rhodamine B
Rhodamine 640	630	621 .. 674	14 %	Ethanol	0.50	Rhodamine 101
DCM	640	605 .. 665	13 %	Ethanol	0.30	
LDS 698	693	664 .. 722	9 %	Ethanol	0.45	Pyridine 1

In summary, the following procedure has to be followed for the difference mixing scheme (Figure A.1.4). First, for $\boldsymbol{\omega_1}$, the 202.3 nm (6.13 eV; ω_1) light was generated utilizing a dye laser (Sirah, Cobra-Stretch; 350–630 nm) containing a dye mixture of Rh 610 and Rh 640 dye (Exciton) in ethanol, which was pumped by the second harmonic (532 nm; 2.33 eV) of the fundamental of a Nd:YAG laser (1064 nm; 1.17 eV; Spectra Physics, PRO-270-30). The dye laser output was frequency tripled (THG) from the fundamental wavelength (606.9 nm; 2.04 eV) – using a β-BaB_2O_4 (BBO) crystal (77°) (Table A.1.3). Second, for $\boldsymbol{\omega_2}$, the 466.7 nm (2.66 eV; ω_2) light was produced by using the third harmonic (354.6 nm; 3.49 eV) of the 1064 nm (1.17 eV) fundamental of a Nd:YAG laser (Spectra Physics, PRO-250-30) at a power of 333 mJ $pulse^{-1}$ to pump a dye laser (Sirah, Precision Scan; 400–900 nm) containing Coumarin 460 dye in ethanol yielding 30 mJ per pulse (Figure A.1.3). Peak efficiencies of 25 % for 532 nm pumped dyes and 15 % for 355 nm pumped dyes are typical (Figure A.1.3, Table A.1.4).

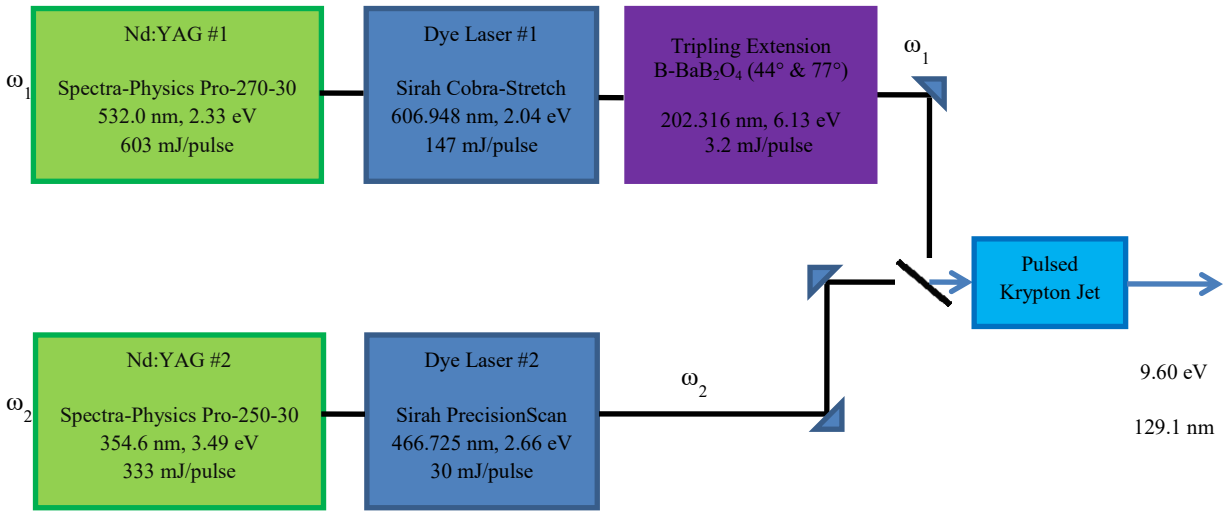

Figure A.1.4. Top view schematic of the pulsed laser system used in the generation of tunable VUV at 129.1 nm (9.60 eV) utilizing resonant four-wave difference mixing ($2\omega_1 - \omega_2$; ω_1 = 202.3 nm; ω_2 = 466.7 nm).

STEP 4:

Now that an acceptable VUV generation scheme has been chosen, the respective Nd:YAG and Sirah dye laser manuals should be consulted for correct operation to produce the necessary wavelengths as determined from the previous steps.

1. Review the Nd:YAG operation manual to ensure safe operation and correct alignment procedures.
2. Set the respective Nd:YAG laser to produce either 532 or 355 nm as determined from which dye was chosen for each dye laser (Table A.1.1 & Figure A.1.3).
3. Review the respective Sirah dye laser manual to ensure safe operation and correct alignment procedures.
4. Initially set the dye laser grating to the maximum output for the selected dye until a laser beam is achieved and then adjust the wavelength with the Sirah software to the desired wavelength.
5. Check that the output wavelength is correct with the wavemeter and its respective photodiode.
6. Install any BBO crystals into the doubling and/or tripling sections of the dye lasers, consulting the dye laser manual for correct installation and alignment procedures.

STEP 5:

Once the ω_1 and ω_2 light has been generated, they need to be spatially and temporally overlapped, and aligned into the vacuum chamber (Figure A.1.5).

1. Use dichroic mirrors to align the ω_1 light into the pulse valve chamber, by centering them through two fixed apertures attached at the edge of the laser table.
2. If available use dichroic mirrors to align the ω_2 light into the pulse valve chamber – UV grade fused silica 90° prisms are also acceptable for this wavelength typically – by centering them through the two fixed apertures.
3. Temporally align the ω_1 and ω_2 light by monitoring their signals on a photodiode connected to an oscilloscope and adjusting their respective flashlamp channel delays (Channels A and E; Figure A.1.5) until their signals occur at an overlapping time.

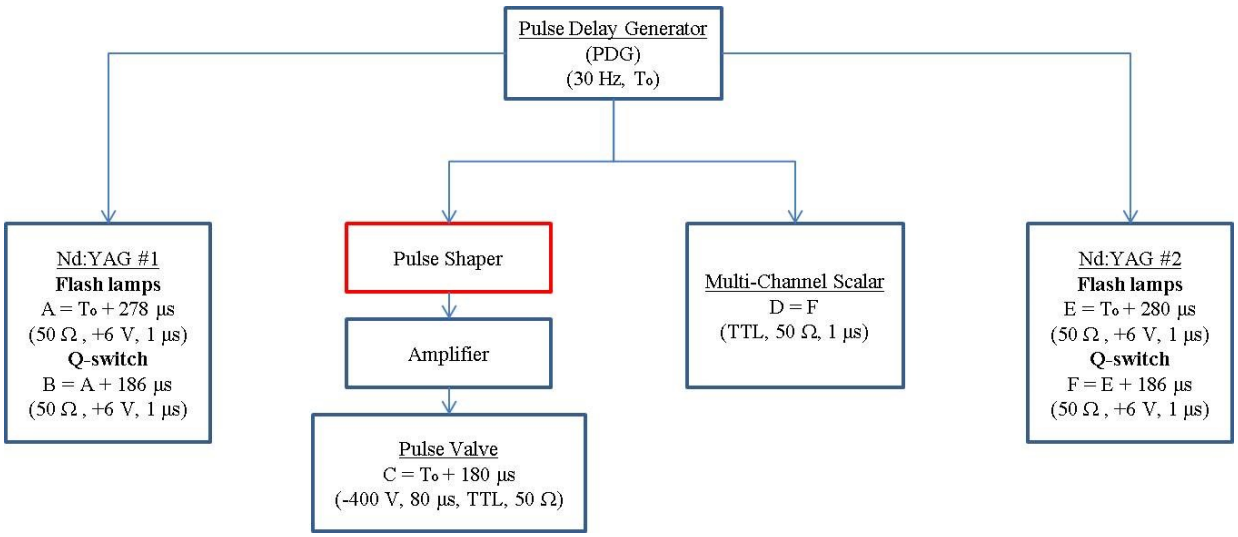

Figure A.1.5. Schematic of the pulse sequence of the single photon photoionization reflectron time-of-flight mass spectrometer relative to the starting pulse operating at 30 Hz.

STEP 6:

The overlapped beams are then focused via a UV grade fused silica plano-convex lens (f = 300 mm at 355 nm) through a UV grade fused silica window into a T extension connected to a pulsed valve.

1. Determine the focal length for ω_1 from the UV grade fused silica convex lens and adjust the position of the lens so that the distance from the lens to the pulse valve is approximately the focal length distance.
2. Allow the selected gas (krypton or xenon) into the pulse valve feedlines and turn on the pulse valve to operate so that the pressure for this chamber is about 1×10^{-4} Torr.
3. Check that there is no ablation of the pulse valve and utilize the x-y-z translatable stage of the lens to correct this if ablation is observed.

A description of these steps for the generation of 9.60 eV follows. Then, both ω_1 and ω_2 were focused by exploiting a UV grade fused silica convex lens and were introduced through a UV grade fused silica window into a differentially pumped vacuum chamber, which houses a pulsed piezoelectric valve. The lens is mounted to an x-y-z translatable stage for precise movements as the pulse valve inlet has a 1 mm aperture. Here, the x and y translate in the horizontal and vertical direction, respectively. The z translation allows for the lens to moved further or closer to the entrance window, which allows for adjustment of the point to which the input wavelengths

are being focused into the pulse valve. The pulsed valve operates at a backing pressure of about 1500 Torr, pulse widths of 80 μs, a repetition rate of 30 Hz, and introduced pulsed jets of krypton (99.999 %; Specialty Gases), which serves as a non-linear medium to generate the 9.60 eV VUV photons via resonant difference four-wave mixing from the photons of the spatially and temporally overlapping ultraviolet (202.316 nm; 6.13 eV; ω_1) and visible (466.725 nm; 2.66 eV; ω_2) laser beams.

STEP 7:

The light passing through/produced in the gas is then separated with a lithium fluoride (LiF) bi-convex lens based on the relative refractive index (A.3).

1. Adjust the micrometer screws on either side of the LiF lens housing to push the lens in the horizontal direction until a signal is observed on the detector via an oscilloscope. Note that the faraday cup detector has a voltage of 310 V applied and this power supply must first be switched on.
2. Typically both the ω_1 and ω_2 light is able to be observed with the faraday cup and can be further aligned to the detector via the dichroic mirrors, UV prisms, and UV convex lens to ensure optimal overlap of the beams.
3. Shift the LiF lens to the left, relative to the input of the laser beams, by tightening the right-side micrometer screw and loosening the left-side micrometer screw (Figure A.1.6) to search for the VUV signal from the position at which ω_1 light is detected.
4. To check if an observed signal is VUV simply turn off the pulse valve or block a single input wavelength, and if the signal decreases after performing either of these options the signal is due to VUV.
5. Optimize the pulse valve region pressure with respect to the VUV signal by adjusting the backing pressure, pulse width, and operating pressure.
6. Optimize all optical elements (dichroic mirrors, UV prisms, UV convex lens, LiF lens)
7. Optimize all possible timing delays (Nd:YAGs, pulse valve).
8. Repeat steps 5-7 several times to ensure optimization of all parameters.

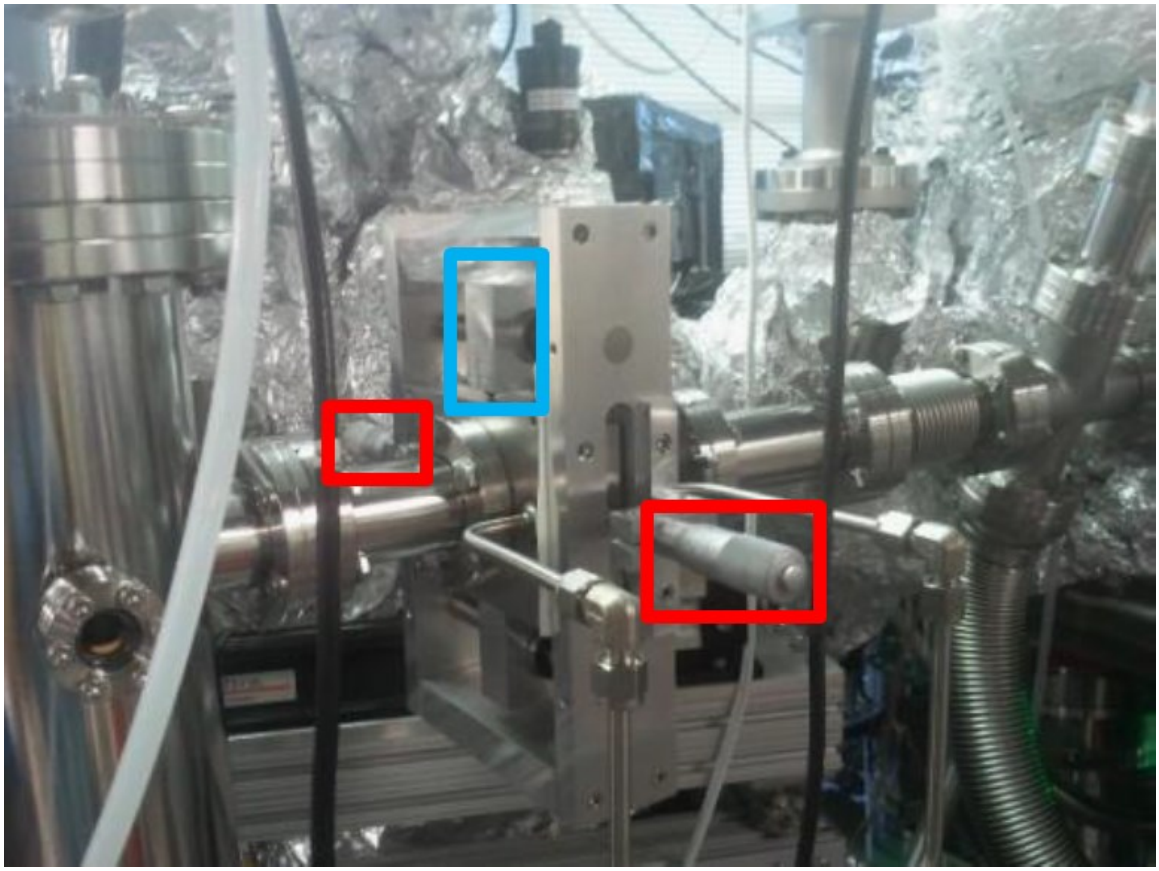

Figure A.1.6. Image of the LiF housing attached to the vacuum chamber with the micrometer screw used to shift the lens horizontally shown in red boxes and vertical adjustment shown in the blue box.

A top-down schematic of the laser setup for 9.60 eV production is depicted in Figure A.1.7. Note that this process generates ultraviolet light (202.3 nm, 6.13 eV, ω_1), visible light 466.7 nm, 2.66 eV, ω_2), and VUV light (83.1 nm, 14.92 eV, $2\omega_1 + \omega_2$; 129.15 nm, 9.60 eV, $2\omega_1 - \omega_2$; 67.4 nm, 18.39 eV, $3\omega_1$; 155.6 nm, 7.98 eV, $3\omega_2$), which in principle can all photoionize subliming molecules. The desired 9.60 eV photons are separated from the 'unwanted' light by using an off axis LiF bi-convex lens.[4] Lithium fluoride does not transmit light above 105 nm (11.80 eV) thus absorbing the 14.92 eV and 18.39 eV light. Further, since the LiF lens has distinct refractive indices for different wavelengths, the off-axis location of the lens with respect to the incident photon beams results into an angular separation of the 155.6 nm (7.98 eV, $3\omega_2$), 202.3 nm (6.13 eV, ω_1), and 466.7 nm (2.66 eV, ω_2) light, i.e. by 6.2 mm, 10.6 mm, and 15.1 mm from the focused 129.15 nm (9.60 eV, $2\omega_1 - \omega_2$) at a distance of 525 mm from the pulsed valve (section A.3). The LiF lens is also able to be translated in the horizontal and vertical position using

micrometer screws which allows for the alignment of the desired wavelength into the main chamber. The 129.15 nm (9.60 eV, $2\omega_1 - \omega_2$) light then passes through a 1 mm aperture of a ceramic plate and photoionizes the subliming molecules about 1 mm above the silver substrate.

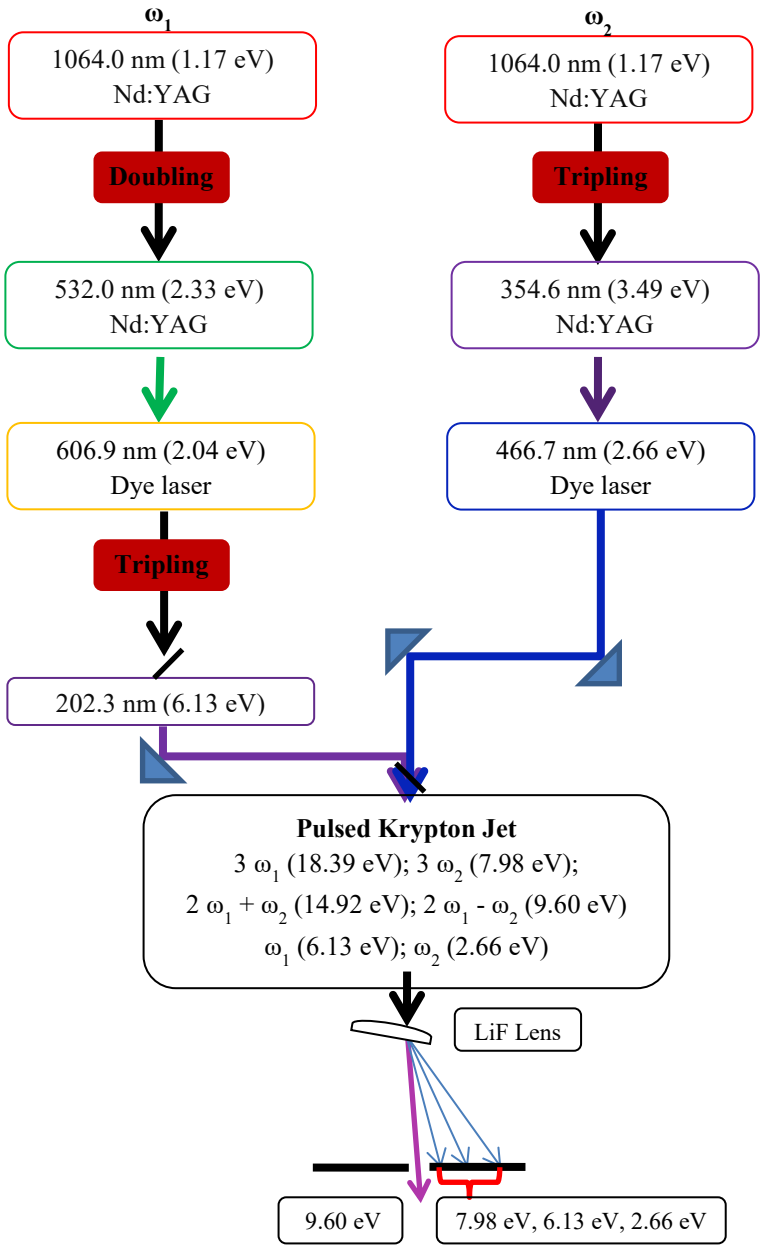

Figure A.1.7. Flow diagram depicting the necessary wavelengths and optical components for the generation of coherent tunable vacuum ultraviolet light at 129.1 nm (9.60 eV) using resonant four-wave difference mixing.

STEP 8:

Two detectors were used to monitor and to optimize the generated VUV light and to ensure proper alignment of the VUV light through the main chamber. The first detector, a faraday cup, operates on the photoelectric principle and was constructed of high purity oxygen free high conductivity copper (OFHC) consisting of one solid disk with a diameter of 1.25 cm and thickness of 0.38 cm coupled to a ring with an inner diameter of 0.5 cm and separated using ceramic insulators.[1] The alternate detector is a NIST calibrated photodiode (Opto. Diode Corp. SXUV100) utilized to characterize the flux of the VUV light. These detectors are mounted on a translatable arm within the system so only one detector can be used at a time and must be aligned to the VUV light. The intensity of the VUV light was measured online during the experiment with the faraday cup type detector.

A.2 Four-Wave Mixing

To describe this process mathematically, first the non-linear susceptibility (polarization density, P) of a material must be defined. The electric field component (E) of light passing through a polarizable material (BBO crystals, krypton or xenon gas) is considered (equation A.2.1).[5, 6]

(A.2.1) $$\frac{\partial^2}{\partial z^2}E(z,t) = \nabla^2 E - \left(\frac{n^2}{c^2}\right)\frac{\partial^2 E}{\partial t^2} = \left(\frac{1}{\varepsilon_0 c^2}\right)\frac{\partial^2}{\partial t^2}\mathrm{P}$$

The first steps in solving the wave equation interacting with a non-linear medium show that this interaction is relatable to its refractive index (n) and the speed of light (c), the electric permittivity of free space (ε_0), and polarization density (P). When an intense electromagnetic wave, such as a laser pulse, interacts with polarizable media, higher order non-linear terms can arise for the polarization density (equation A.2.2).

(A.2.2) $$\mathrm{P} = \varepsilon_0(\chi^{(1)}\mathrm{E} + \chi^{(2)}\mathrm{E}^2 + \chi^{(3)}\mathrm{E}^3 + \ldots + \chi^{(n)}\mathrm{E}^n)$$

Here, the polarization density (P) is determined by the static dipole moment of the material (P_0), electric permittivity of free space (ε_0), electric susceptibility (χ), and electric field (E). A linear response ($P = \varepsilon_0\chi^{(1)}E$) is observed as well as multiple non-linear ($\chi^{(n)}E^n$) terms from this interaction. When an isotropic medium (x = -x; y = -y; z = -z), such as krypton or xenon gas, is

utilized as the non-linear material, the susceptibility tensor (χ) is invariant to inversion. Therefore, applying the inversion operator ($\hat{I}_{op}$) to equation A.2.2 shows that only odd non-linear terms are altered (equation A.2.3).

(A.2.3) $\hat{I}_{op} E = -E;\ \hat{I}_{op} P = -\varepsilon_0(\chi^{(1)}E + \chi^{(2)}EE + \chi^{(3)}EEE + \ldots) = \varepsilon_0(-\chi^{(1)}E + \chi^{(2)}E^2 - \chi^{(3)}E^3 + \ldots)$

Due to the polarization density remaining equivalent for even ordered terms ($P^{(2n)} = - P^{(2n)}$), the electric susceptibility (χ) must equal zero for the even ordered non-linear terms, and therefore the even ordered non-linear terms are not produced in isotropic media (equation A.2.4).

(A.2.4) $P = \varepsilon_0(\chi^{(1)}E + \chi^{(3)}E^3 + \chi^{(5)}E^5 + \ldots + \chi^{(2n+1)}E^{2n+1})$

By including the mathematical representation for an electromagnetic wave (equation A.2.5) the output for each term can be calculated for an incident wavelength, for example the third order term (equation A.2.6).

(A.2.5) $E(t) = E\cos(\omega t) = \frac{1}{2}E(e^{i\omega t} + e^{-i\omega t})$

(A.2.6) $P^{(3)} = \varepsilon_0\chi^{(3)}(\ ½Ee^{i\omega t} + ½Ee^{-i\omega t})^3 = \varepsilon_0\chi^{(3)}E^3(\frac{1}{8}e^{-3i\omega t} + \frac{1}{8}e^{3i\omega t} + \frac{3}{8}e^{i\omega t} + \frac{3}{8}e^{-i\omega t})$

This method is utilized for the non-resonant four-wave mixing to produce 118 nm light, which is equivalent the frequency tripling (3ω) of 355 nm light (ω) in xenon gas (equation A.2.6). When two input wavelengths (equation A.2.7) are introduced, the third harmonic produces additional waves (equation A.2.8)

(A.2.7) $E = ½E_1e^{-i\omega_1 t} + ½E_1e^{i\omega_1 t} + ½E_2e^{-i\omega_2 t} + ½E_2e^{i\omega_2 t}$

(A.2.8a) $P^{(3)} = \varepsilon_0\chi^{(3)}E^3$

(A.2.8b) $P^{(3)} = \varepsilon_0\chi^{(3)}[\frac{1}{8}E_1^3 e^{\pm i3\omega_1 t} + \frac{1}{8}E_2^3 e^{\pm i3\omega_2 t} + \frac{3}{8}E_1^2E_2 e^{it(2\omega_1\pm\omega_2)} + \frac{3}{8}E_1E_2^2 e^{it(2\omega_2\pm\omega_1)} + \frac{3}{8}E_1^3 e^{\pm i\omega_1 t} + \frac{3}{8}E_2^3 e^{\pm i\omega_2 t} + \frac{3}{4}E_1^2E_2 e^{\pm i\omega_2 t} + \frac{3}{4}E_1E_2^2 e^{\pm i\omega_1 t})$

Here we see that two incoming waves produce several new waves (equation A.2.8b). The first and second terms of equation A.2.8b contain the frequency tripled output of their respective inputs ($3\omega_1$, $3\omega_2$). Also, the third and fourth terms contain the waves corresponding to the sum and difference ($2\omega_1\pm\omega_2$; $\omega_1\pm2\omega_2$) four-wave mixing processes. Finally, the remaining terms contain waves corresponding to the input frequencies. The difference four-wave mixing process was utilized throughout the dissertation. Also, the selection of ω_1 to be resonant with the non-linear gas medium greatly enhances the intensity of the difference frequency only produced from $2\omega_1\pm\omega_2$, and all other light is significantly less intense. Although higher order terms are technically produced, their intensity is significantly reduced compared to the third order terms.[2, 7-10]

A.3 Separation of Tunable Vacuum Ultraviolet Light

The separation of the different wavelengths, such as the input wavelength(s) and four-wave mixing output wavelengths, was accomplished via a LiF lens (Figure A.3.1). This separation is due to the difference in refractive index of each wavelength respective to the LiF material. This can be mathematically represented by manipulating the lens makers' equation for a biconvex lens to determine the deviation of each wavelength through the biconvex LiF lens (equation A.3.1)

(A.3.1) $$\Delta\theta = 2 \times R_{off} \times R_{lens}^{-1} \times (n_2 - n_1)$$

Here, the angular dispersion ($\Delta\theta$) between the two beams can be calculated if the refractive index for the wavelengths of interest (n_1, n_2) are known, along with the radius of curvature of the lens (R_{lens} = 131 ± 3 mm), and finally the distance from the center of the lens (R_{off} = 13 ± 3 mm) that the collinear incident wavelengths passed through the lens. The angular dispersion can be converted to a separation distance (Δx) between the two wavelengths via the trigonometric equation A.3.2.

(A.3.2) $$\Delta x = A \times \tan(\Delta\theta)$$

The distance from the LiF lens to the ceramic exit aperture (A = 525 ± 5 mm), where the unwanted light is blocked, is used to determine the separation of the different wavelengths. For example the separation of the non-resonant four-wave mixing VUV light at 118 nm from the input 355 nm light can be determined from the above equations and constant values as the refractive index of 118 nm and 355 nm light through LiF is measured to be 1.6 ± 0.1, and 1.4 ± 0.1, respectively. This results in a separation of 21 ± 5 mm of the two wavelengths. In Figure A.3.1 the red dashed line shows the path of the center of the incident light before and after the LiF lens as if the lens was not present to show the change in the light's path that the LiF lens induces. The green dashed lines show the center of the incident of higher wavelength (355 nm) is refracted less that the lower wavelengths (blue line; 118 nm). The center of these wavelengths is identical until interaction with the LiF lens. The center of the LiF lens is depicted with a black dotted line. The solid black lines with the blue line passing between them represent a ceramic beam dump installed in the vacuum chamber to block the unwanted wavelengths.

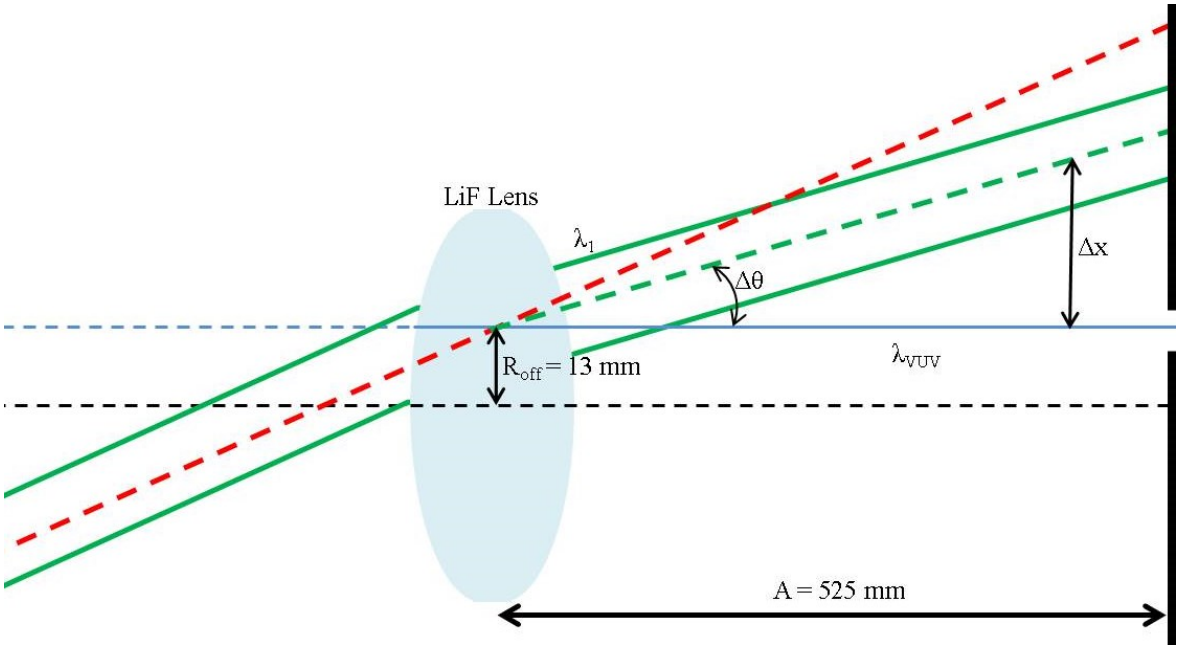

Figure A.3.1. Geometry of the wavelength separation system. The initial light path is traced in red, and the altered paths of the VUV and input wavelengths are shown in green and blue, respectively. See text for details.

References and Notes

1. S. Maity, R. I. Kaiser and B. M. Jones, *Faraday Discuss.*, 2014, **168**, 485-516.
2. R. Hilbig, G. Hilber, A. Lago, B. Wolff and R. Wallenstein, 1986.
3. J. W. Hepburn, *Laser Techniques in Chemistry*, Wiley, New York, NY, 1994.
4. W. A. VonDrasek, S. Okajima and J. P. Hessler, *Appl. Opt.*, 1988, **27**, 4057-4061.
5. R. W. Boyd, in *Nonlinear Optics (Second Edition)*, ed. R. W. Boyd, Academic Press, San Diego, 2003, DOI: https://doi.org/10.1016/B978-012121682-5/50003-1, pp. 67-127.
6. R. W. Boyd, in *Nonlinear Optics (Second Edition)*, ed. R. W. Boyd, Academic Press, San Diego, 2003, DOI: https://doi.org/10.1016/B978-012121682-5/50002-X, pp. 1-65.
7. R. Hilbig and R. Wallenstein, *Quantum Electronics, IEEE Journal of*, 1983, **19**, 194-201.
8. R. Hilbig and R. Wallenstein, *Appl. Opt.*, 1982, **21**, 913-917.
9. H. H. Fielding, Q. Hong, S. Solans, A. J. Langley, S. Schlorholz, W. Shaikh and P. F. Taday, *Optics Communications*, 1996, **123**, 129-132.
10. J. Reintjes, S. Chiao-Yao and R. Eckardt, *Quantum Electronics, IEEE Journal of*, 1978, **14**, 581-596.